Journal of Scientific and Innovative Research 2020; 9(4): 90-96
Available online at: www.jsirjournal.com

Research Article

ISSN 2320-4818
JSIR 2020; 9(4): 90-96

Received: 16-11-2020
Accepted: 07-12-2020

Mohamed K. El-Ashrey
Department of Pharmaceutical Chemistry, Faculty of Pharmacy, Cairo University, Cairo, Egypt

Fatma Elshibani
Department of Pharmacognosy, Faculty of Pharmacy, University of Benghazi, Benghazi, Libya

Abdullah Alamami
Department of Basic Medical Science, Faculty of Pharmacy, University of Benghazi, Benghazi, Libya

Naema Elremali
Department of Pharmaceutical Chemistry, Faculty of Pharmacy, University of Benghazi, Benghazi, Libya

Mahmoud A. Elderbi
Department of Pharmacology, Faculty of Medicine (Almarj), University of Benghazi, Libya

Correspondence:
Dr. Fatma Elshibani
Department of Pharmacognosy, Faculty of Pharmacy, University of Benghazi, Benghazi, Libya
Email: balsmafifahana@yahoo.com

Prediction of Sars-Cov-2 Main Protease Potential Inhibitors from Libyan Arbutus Pavarii Pampan Compounds: A Molecular Docking Study

Mohamed K. El-Ashrey, Fatma Elshibani, Abdullah Alamami, Naema Elremali, Mahmoud A. Elderbi*

Abstract

The present study examined some natural active compounds contained in the Libyan *Arbutus pavarii* Pampan. shrub that might be used as natural inhibitors of SARS-CoV-2, the responsible causative agent of coronavirus disease 2019 (COVID-19). A molecular docking method was employed to find out the capability of the selected molecules to interact with the virus main protease. Seven flavonoids from twenty-seven compounds belonging to different classes showed a remarkable ability to bind to the main protease of the novel coronavirus. The descending order of compounds with the highest binding affinity was as follows: Saponarin, Rutin, Delphinidin-3-rutinoside, Neodiosmin, Kampferol-3-O-ß-D-rutinoside, Isoquercetin, and Hyperoside. The outcomes have provided a clear insight into the structure-activity relationship of Mpro targeting agents and may assist the future design of new drug candidates for the disease.

Keywords: COVID-19, Libyan *Arbutus pavarii*, Molecular docking, Flavonoids.

INTRODUCTION

The family of viruses that infect the human respiratory system involves several strains of coronaviruses with SARS-CoV-2 being the most virulent that can cause massive mortalities once transmitted among populations [1]. Coronavirus disease 2019 (COVID 19) emergence was in the form of severe pneumonia symptoms spreading fast in Wuhan, China at the end of December 2019 [2-5].

SARS-CoV-2 is a single-stranded positive-sense RNA virus, containing membrane, envelope proteins, and spikes. The analysis of the viral genetic material manifested that its genome includes ~30,000 nucleotides comprising essential replicase gene that encodes pp1a and pp1ab, which are overlapping poly-proteins [4,5]. 3CLpro is one of the chief enzymes of SARS-CoV-2, which is also recognized as the main protease (Mpro) that has a fundamental role in the multiplication of the virus by cleaving the poly-protein at eleven distinct sites to produce non-structural proteins that are essential to the step of replication [6]. Accordingly, the protein is considered as a significant target in the screening for anti-coronaviruses [7]. Furthermore, this viral key enzyme undergoes autocatalytic cleavage of itself and the human host does not have any close homologs. Consequently, using a suitable protease inhibitor to block the action of this enzyme holds a huge potential to limit the process of replication and transcription, which are crucial steps in the life cycle of the virus [8].

For decades, medicinal plants have been a major source for the isolation of bioactive molecules and the discovery of the novel drug. In other words, purified phytochemicals can be employed in the development of more efficient medications based on the structure-activity relationship [9]. Directly after the outbreak of COVID19, few researches concerning the screening for 3CLpro inhibitors of natural origin have been accomplished using computer modeling.

Plant secondary metabolites that are studied in this paper for their anti-coronavirus effect include terpenoids, flavonoids, and phenolic acids.

The attention in the last decade in the direction of the antiviral activity of natural flavonoids has increased because of the frequency of viral infections, which affect several million patients annually, chiefly

influenza infections [10].

The affinity of these compounds to bind to a specific receptor of the target virus protein is investigated by molecular docking assay. The compound that reveals lower binding energy is considered as a potential drug candidate [11].

Arbutus pavarii Pamp (known as the strawberry tree) is an evergreen shrub belongs to the *Ericaceae* family. The plant is used as a diuretic, antiseptic, laxative, and for the management of arterial hypertension [12]. According to some previous studies, the extracts of the aerial parts could be used as antimicrobial, antioxidant, and cytotoxic agents [13]. The species is endemic in Gebal Al-Akhdar, east of Libya (The Green Mountain) [12].

Various compounds belong to the classes of phenolic acids, flavonoids and tri-terpenoids were isolated from the aerial parts of the *Arbutus pavarii* Pampan, including *β*-amyrin acetate, catechin, lupeol, salicylic acid, kaempferol, Methyl gallate**,** gallic acid, ferulic acid, arbutin, isoquercetin, quercetin 3-O-β-D-galactopyranoside (Hyperoside), Kampferol-3-O-*β*-D-rutinoside**,** dioctyl phthalate, and neochlorogenic acid. Moreover, isovitexin-7-O-glucoside (Saponarin**)**, neodiosmin, naringenin-7-O-glucoside, quercetin, dihydroquercetin, and rutin were identified in the same plant as major flavonoids. Five phenolic acids comprising rosmarinic, gallic, caffeic, chlorogenic, and salicylic acids, as well as one anthocyanin; delphinidin-3-O-rutinoside, and one carboxylic acid; quinic acid, were also recognized [14].

Other study showed that, among the flavonoids identified and determined by HPLC analysis, rutin, epiactetchin and hesperidine were found most abundant in Arbutus pavarii Pampan methanolic extract [15].

In the present investigation, a computational study was conducted on a previous library of phytochemicals, which are isolated and identified from one of the endemic promising Libyan medicinal plants to screen for potential inhibitors of 3CLpro, which eventually can be utilized as novel molecules to accelerate the rate of designing anti-COVID-19 drug candidates.

MATERIAL AND METHODS

Molecular docking study

Molecular Operating Environment (MOE, 2019.0102) software was used to carry out all the molecular modeling studies. All minimizations were performed by MOE until a root-mean-squared-deviation (RMSD) gradient of 0.05 kcal·mol^{-1}Å^{-1} with the MMFF94x force field and the partial charges were automatically calculated.

Preparation of the target (SARS-CoV-2 main protease Mpro):

The X-ray crystallographic structure of the main protease enzyme in SARS-COV-2 co-crystallized with its bound ligand X77 (PDB ID: 6W63) was downloaded from the protein data bank (https://www.rcsb.org/structure/6W63). For each co-crystallized enzyme, ligands and water molecules that are not involved in the binding were removed. The protein was prepared for the docking study using *Protonate 3D* protocol in MOE with default options. The co-crystalized ligand (X77) was used to define the binding site for docking [16].

Docking of the affinity of tested molecules to viral main protease binding site:

Docking of the previously mentioned database composed of twenty-seven test compounds and the co-crystallized inhibitor X77 was performed. The following method was carried out; the file of the prepared enzyme active site was loaded and a general docking process was applied. The specifications of the program were adjusted; the docking site was specified as dummy atoms, triangle matcher as the placement methodology, and the scoring method was London dG. Rigid receptor as refinement methodology and the scoring method GBVI/WSA dG for the selection of the best twenty poses from two-hundred different poses for each tested compound. The scoring methodologies were adjusted to the default values. The ten ligands MDB file was loaded and general dock calculations were run automatically. After finishing the processes of docking, the obtained poses were observed and the best ones revealing the highest ligand–enzyme interactions and the best acceptable RMSD values were chosen and saved for energy calculations. A validation process was also performed at the beginning for the target protease by running the process of docking only for the co-crystallized ligand and low RMSD values between docked and crystal conformations that indicate valid performance [17,18].

RESULTS

The docking results are summarized in Table (1).

Through the investigation of the binding interactions of X77 to the active site of the enzyme, it shows H-bond interactions with the key amino acids Thr26, Met49, Asn142, Gly143, Cys145, His163, His164, and Glu166 (Figure 1).

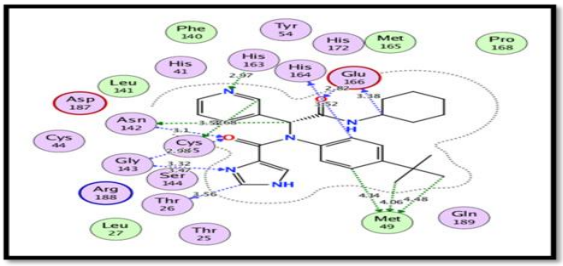

Figure 1: 2D interactions of X77 within SARS-COV-2 main protease active site

The docking setup was first validated by self-docking of the co-crystallized ligand (X77) in the vicinity of the binding site of the enzyme, the docking score (S) was -8.5061 kcal/mol. and root mean square deviation (RMSD) was 1.0543 Å indicating the validation of the docking process (Figure 2).

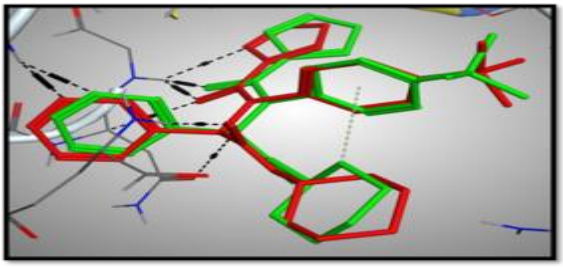

Figure 2: 3D representation of the superimposition of the co-crystallized (red) and the docking pose (green) of X77 in the SARS-COV-2 main pro tease active site

The validated setup was then used in predicting the ligand-receptor interactions at the binding site for the compounds of interest.

DISCUSSION

Several studies have reported the anti-coronavirus effect of flavonoid compounds through the molecular docking of the molecules to the main protease domain.

The results suggested that three of the studied compounds belonging to different classes of flavonoid have exhibited a higher binding score than the co-crystallized ligand (X77); Saponarin, Rutin, and Delphinidin-3-rutinoside (-8.7321, -8.6309 & -8.5644, respectively) have strongly bound to the main protease active site through H-bond and electrostatic interactions compared to the bound ligand. According to the MolDock binding score, these active constituents could be potential inhibitors of COVID-19 protease especially Saponarin which was posed correctly into the enzyme active pocket with the formation of five H-bonds with Met49, Met165 and Gln192, followed by Rutin (Figures 3-5).

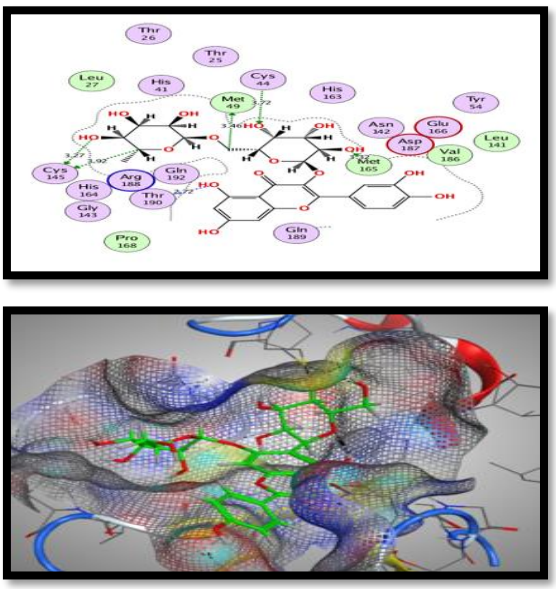

Figure 3: 2D & 3D diagram of compound Saponarin interactions withing SARS-COV-2 main protease active site

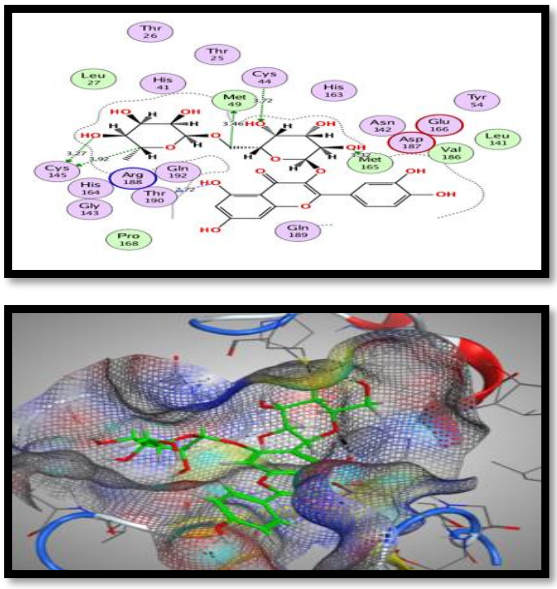

Figure 4: 2D & 3D diagram of compound Rutin interactions withing SARS-COV-2 main protease active site

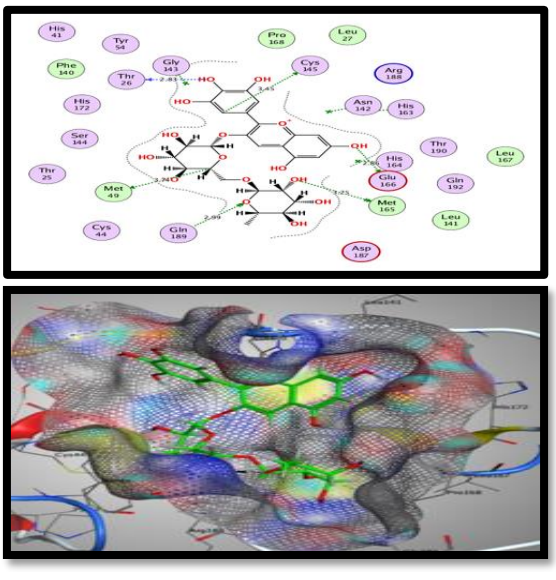

Figure 5: 2D & 3D diagram of compound Delphinidin-3-rutinoside interactions withing SARS-COV-2 main protease active site

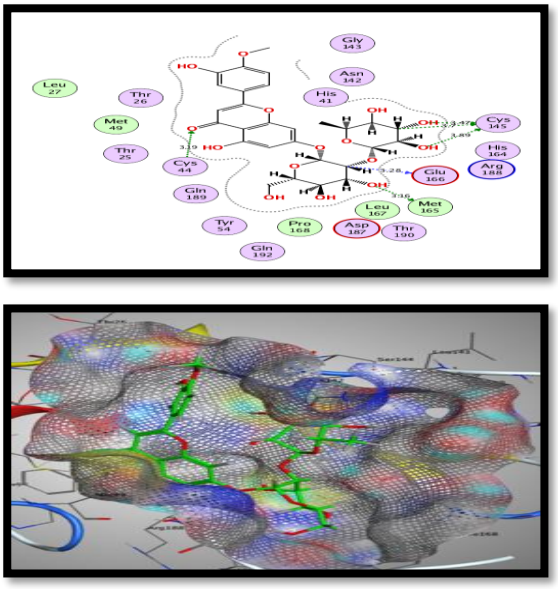

Figure 6: 2D & 3D diagram of compound Neodiosmin interactions withing SARS-COV-2 main protease active site

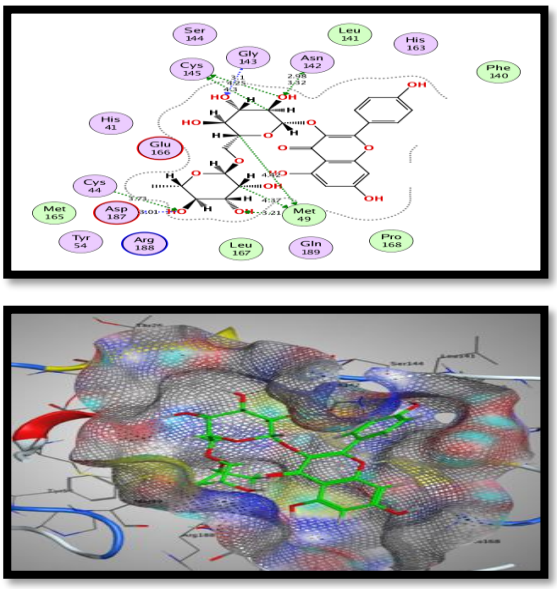

Figure 7: 2D & 3D diagram of compound Kampferol-3-O-ß-D-rutinoside interactions withing SARS-COV-2 main protease active site

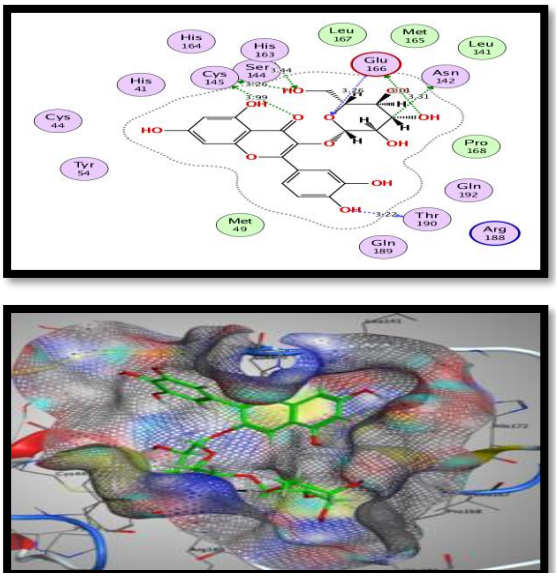

Figure 8: 2D & 3D diagram of compound Isoquercetin interactions withing SARS-COV-2 main protease active site

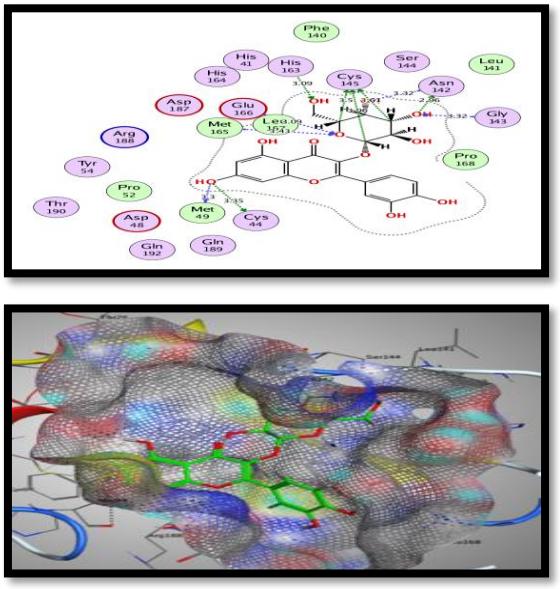

Figure 9: 2D & 3D diagram of compound Hyperoside interactions withing SARS-COV-2 main protease active site

The compounds belong to the flavonoid chemical class, which accounts for a large part of polyphenolics and have high medical values due to their antioxidant activity without any noticeable adverse effects reported. Some other studies confirmed their antibacterial, antifungal, and antiviral properties [19].

Saponarin is isovitexin-7-O-glucoside can be found in young green barley leaves and possess a potent antioxidant capacity [20], whereas rutin is an essential nutritional component of apples, tea, and citrus plants [21,22]. It has been found to have antioxidant, anti-inflammatory and anti-free radical effects [23].

Recent molecular docking research showed that rutin has a significant inhibitory effect against SARS-CoV-2 Mpro, which supports the current results of this study [24,25].

Interestingly, delphinidin-3-rutinoside has been found as a main anthocyanin glucoside in berries and leaves of black currant (*Ribes nigrum* L.) [26], also obtained from extracts of *Solanum Melongena* L. (Solanaceae), inhibited herpes simplex virus strain HSV-1 replication [27].

The other tested compounds displayed good binding score and good binding interactions; Neodiosmin, Kampferol-3-O-ß-D-rutinoside, Isoquercetin, and Hyperoside have scores of -8.2242, -7.9048, -7.5212, and -7.2587 respectively, which are significant outcomes, hence they can be considered as promising COVID-19 Mpro inhibitors. Their modes of binding are illustrated in (Figures 6-9). Neodiosmin is a flavone glycoside found in limes and can be obtained from the dehydrogenation process of neohesperidin. The compound possessed antiviral properties through the inhibition of SARS-CoV-2 Mpro as indicated by a similar previous study [28]. Furthermore, it was demonstrated that iso-quercetin and hyperoside that extracted from Nymphaea alba L. (Nymphaeaceae), exhibits anti-HCV (hepatitis C virus) activity through suppressing NS3 gene expression [29].

Table 1: Docking results

Compound	S (kcal/mol)	Amino acids	Interacting groups	Type of interaction	Length
X77	-8.5061	Thr26	CH (imidazole)	Electrostatic	3.56
		Met49	CH_3 (tert.butyl)	Electrostatic	4.06
		Met49	CH_3 (tert.butyl)	Electrostatic	4.48
		Met49 Asn142	CH (benzene)	Electrostatic	4.14
		Asn142	CH	Electrostatic	3.52
		Gly143	O (C=O)	H-bond acceptor	3.10
		Gly143	O (C=O)	H-bond acceptor	2.98
		Cys145	N (imidazole)	H-bond acceptor	3.32
		His163 His164	CH (pyridine)	Electrostatic	2.68
		Glu166	N (pyridine)	H-bond acceptor	2.97
			CH (benzene)	Electrostatic	3.52
			CH (cyclohexyl)	Electrostatic	3.38
Acacetin	-5.8751	Phe140	OH	H-bond donor	3.05
		Cys145	O (C=O)	H-bond acceptor	3.65
		Cys145	CH (pyran)	Electrostatic	3.53
		Cys145	CH (benzene)	Electrostatic	4.27
		His163	O (C=O)	H-bond acceptor	3.10
Arbutin	-5.8093	Met49	OH	H-bond donor	3.42
		Met165	CH (benzene)	Electrostatic	3.62
Caffeic acid	-4.8368	Cys145	OH	H-bond donor	3.28
		His164	OH	H-bond donor	3.45
		Glu166	OH (acid)	H-bond donor	3.14
Catechin	-5.9229	Met49	OH	H-bond donor	4.34
		Met49 Met49	CH	Electrostatic	4.03
		Asp187	CH_2	Electrostatic	3.89
			OH	H-bond donor	2.97
Chlorogenic acid	-7.1211	Cys44	O (C=O)	H-bond acceptor	3.64
		Met49	OH	H-bond donor	3.36
		Phe140	OH	H-bond donor	4.32
		Met165	OH (phenolic)	H-bond donor	3.02
Delphinidin-3-rutinoside	-8.5644	Thr26	OH	H-bond donor	2.83
		Met49	CH	Electrostatic	3.74
		Cys145	CH (benzene)	Electrostatic	3.45
		Met165	OH	H-bond donor	3.25
		Glu166	OH	H-bond donor	2.86
		Gln189	O (pyran)	H-bond acceptor	2.99
Dihydrokampferol	-5.8762	Asn142	OH	H-bond donor	3.31
		Cys145	OH	H-bond donor	3.53
		Glu166	OH	H-bond donor	3.08
		Asp187	OH	H-bond donor	2.96

Dihydroquercitin	-5.9876	Cys145	OH	H-bond donor	3.26
		Glu166	CH	Electrostatic	3.13
		Arg188	OH	H-bond donor	3.11
Dioctyl phthalate	-7.9464	Cys145	CH_3	Electrostatic	3.78
		Cys145	CH_2	Electrostatic	3.61
		Met165	O (C=O)	H-bond acceptor	3.61
		Met165	CH_3	Electrostatic	4.49
		Met165	CH_2	Electrostatic	3.84
Ferulic acid	-4.9471	Pro168	O C=O)	H-bond acceptor	3.70
		Arg188	OH	H-bond donor	3.10
Gallic acid	-4.7248	Met165	OH	H-bond donor	4.44
		Arg188	OH	H-bond acceptor	3.55
Hyperoside	-7.2587	Cys44	OH (phenolic)	H-bond donor	3.35
		Met49	OH (phenolic)	H-bond donor	3.30
		Asn142	OH	H-bond donor	2.96
		Asn142	OH	H-bond acceptor	3.32
		Gly143	OH	H-bond acceptor	3.32
		Cys145	CH (pyran)	Electrostatic	3.50
		Cys145	CH (pyran)	Electrostatic	3.61
		Cys145	CH (pyran)	Electrostatic	3.96
		His163	OH	H-bond acceptor	3.09
		Met165	O (pyran)	H-bond acceptor	3.43
		Glu166	O (pyran)	H-bond acceptor	3.09
Isoquercetin	-7.5212	Thr190	OH (phenolic)	H-bond donor	3.22
		Asn142	CH (pyran)	Electrostatic	3.31
		Cys145	OH	H-bond donor	3.26
		Cys145	O (C=O)	σ-hole bond	3.99
		His163	OH	H-bond acceptor	3.44
		Glu166	O (pyran)	H-bond acceptor	3.26
		Glu166	OH	H-bond donor	3.01
Kampferol-3-O-ß-D-rutinoside	-7.9048	Cys44	OH	H-bond acceptor	3.73
		Met49	OH	H-bond acceptor	3.21
		Met49	CH	Electrostatic	4.37
		Met49	CH	Electrostatic	4.42
		Asn142	OH	H-bond acceptor	3.32
		Gly143	OH	H-bond acceptor	3.10
		Cys145	OH	H-bond donor	4.25
		Cys145	CH	Electrostatic	4.30
		Asp187	OH	H-bond donor	3.01
Kaempferol	-5.6048	Met49	CH (benzene)	Electrostatic	3.49
		Met165	OH	H-bond donor	4.37
		Asp187	OH	H-bond donor	3.01
Lupeol	-6.1193	Met49	CH_3	Electrostatic	4.48
		Met49	CH_2	Electrostatic	4.00
		Met49	CH	Electrostatic	4.16
		Cys145	CH_3	Electrostatic	4.37
Methyl gallate	-4.8149	Met165	OH	H-bond donor	3.28
Narengenin-7-O-glucoside	-7.2874	Cys44	O (C=O)	H-bond acceptor	3.29
		Met49	CH (pyran)	Electrostatic	4.34
		Met165	CH_2	Electrostatic	3.92
		Gln189	OH	H-bond acceptor	2.85
		Gln192	OH	H-bond acceptor	3.07
Neodiosmin	-8.2242	Cys44	O (C=O)	H-bond acceptor	3.19
		Cys145	OH	H-bond donor	3.47
		Cys145	OH	H-bond donor	3.89
		Cys145	CH (pyran)	Electrostatic	3.70
		Met165	OH	H-bond donor	3.16
		Glu166	CH (pyran)	Electrostatic	3.28
Quercetin	-5.8902	Met165	CH (benzene)	Electrostatic	3.85
		Met165	CH (benzene)	Electrostatic	4.07
		Gln192	OH	H-bond donor	2.90
Quinic acid	-4.5465	Glu166	CH	Electrostatic	3.35
		Gln189	OH	H-bond acceptor	3.08
Rhamnetin	-5.9780	Cys145	OH	H-bond donor	3.80
		Cys145	CH (benzene)	Electrostatic	4.00
		Arg188	OH	H-bond donor	3.37
		Arg188	CH (benzene)	Electrostatic	3.40
Rosmarinic acid	-6.6990	Cys145	OH	H-bond donor	4.35
		Cys145	CH (benzene)	Electrostatic	3.75
		Met165	OH	H-bond donor	3.23
		Met165	O (C=O)	σ-hole bond	3.43
		Glu166	OH	H-bond donor	3.39

Rutin	-8.6308	Cys44	OH	H-bond acceptor	3.72
		Met49	CH_2	Electrostatic	3.46
		Cys145	OH	H-bond donor	3.27
		Cys145	CH	Electrostatic	3.92
		Met165	OH	H-bond donor	3.32
		Thr190	OH	H-bond donor	2.72
Salicylic acid	-4.3148	Met49	OH	H-bond donor	3.53
		Met49	CH (benzene)	Electrostatic	3.88
		Met165	OH	H-bond donor	3.46
		Met165	CH (benzene)	Electrostatic	4.03
Saponarin	-8.7321	Met49	OH	H-bond donor	3.35
		Met49	OH	H-bond donor	3.86
		Cys145	O (C=O)	σ-hole bond	3.11
		Met165	OH	H-bond donor	3.14
		Met165	OH	H-bond donor	3.47
		Gln192	OH	H-bond acceptor	3.18
β-amyrin acetate	-7.0896	Met49	CH_3	Electrostatic	4.21
		Met49	CH_2	Electrostatic	3.91
		Glu166	CH	Electrostatic	3.40

CONCLUSION

This study confirmed the high affinities of the compounds isolated and identified from the aerial parts of *Arbutus pavarii* Pampan. for COVID-19 protease. Accordingly, the findings indicate and clarify the potential effectiveness of the tested compounds against the virus and give primary insights about the structure-activity relationship of Mpro inhibitors to facilitate the future design of new drug candidates to cure the disease.

Conflict of interest

Authors declare no conflict of interest.

REFERENCES

1. Weiss S R. & Navas-Martin S. Coronavirus pathogenesis and the emerging pathogen severe acute respiratory syndrome coronavirus. Microbiology and molecular biology reviews. 2005. 69(4), 635-664.
2. Zhu N. Zhang D. Wang W. Li X. Yang B. Song, J & Niu P. A novel coronavirus from patients with pneumonia in China, 2019. New England Journal of Medicine.2020 .
3. Li Q. Guan X. Wu P. Wang X. Zhou L. Tong Y & Xing X. Early transmission dynamics in Wuhan, China, of novel coronavirus–infected pneumonia. New England Journal of Medicine.2020 .
4. Zhou P. Yang, X L. Wang X G. Hu B. Zhang L. Zhang W & Chen H D. A pneumonia outbreak associated with a new coronavirus of probable bat origin. Nature. 2020. 579(7798), 270-273.
5. Wu F. Zhao S. Yu B. Chen Y M. Wang W. Song, Z G & Yuan M L. A new coronavirus associated with human respiratory disease in China. Nature. 2020. 579(7798), 265-269.
6. Anand K. Ziebuhr J. Wadhwani P. Mesters J R & Hilgenfeld R. Coronavirus main proteinase (3CLpro) structure: basis for design of anti-SARS drugs. Science. 2003.300(5626), 1763-1767.
7. Needle D. Lountos G T & Waugh D S. Structures of the Middle East respiratory syndrome coronavirus 3C-like protease reveal insights into substrate specificity. Acta Crystallographica Section D: Biological Crystallography.2015. 71(5), 1102-1111.
8. Giri S. Lal A F & Singh S. Battle against Coronavirus: Repurposing old friends (Food borne polyphenols) for new enemy (COVID-19).2020 .
9. Mani J S. Johnson J B. Steel J C. Broszczak D A. Neilsen P M. Walsh K B. Naiker M. Natural product-derived phytochemicals as potential agents against coronaviruses: a review. Virus Research. 2020. 197989.
10. Moscona A. Oseltamivir resistance—disabling our influenza defenses. New England Journal of Medicine. 2005. 353(25). 2633-2636.
11. Chandel V. Raj S. Rathi B and Kumar D. In Silico Identification of Potent COVID-19 Main Protease Inhibitors from FDA Approved Antiviral Compounds and Active Phytochemicals through Molecular Docking: A Drug Repurposing Approach. 2020.
12. Hegazy A K. Al-Rowaily S L. Faisal M. Alatar A A. El-Bana M I & Assaeed A M. Nutritive value and antioxidant activity of some edible wild fruits in the Middle East. Journal of Medicinal Plants Research. 2013. 7(15), 938-946.
13. Tenuta M C. Tundis R. Xiao J. Loizzo M R. Dugay A & Deguin B. Arbutus species (Ericaceae) as source of valuable bioactive products. Critical reviews in food science and nutrition. 2019. 59(6), 864-881.
14. El-Shibani, F. A Pharmacognostical study of Arbutus pavarii Pampan. Family Ericaceae and Sarcopoterium spinosum L. Family Rosaceae Growing in Libya. PhD diss. 2017. Cairo University, Cairo.
15. Ezzat S. El-Hawary S. El Shabrawy A & El-Shibani F. Evaluation of the phenolic and flavonoid contents, antimicrobial and cytotoxic activities of some plants growing in Al Jabal Al-Akhdar in Libya., International Journal of Pharmacognosy and Phytochemical Research. 2016. 8(7); 1083-1087
16. Jin Z. Du X. Xu Y. Deng Y. Liu M. Zhao Y. Yang H. Structure of Mpro from COVID-19 virus and discovery of its inhibitors. Nature. 2020. 1-5.
17. Davis I W & Baker D. RosettaLigand Docking with Full Ligand and Receptor Flexibility. Journal of Molecular Biology. 2009. 385(2), 381–392.
18. McConkey B J. Sobolev V & Edelman M. The performance of current methods in ligand-protein docking. Current Science. 2002. 83(7), 845–856.
19. Tapas A R. Sakarkar D M and Kakde R B. Flavonoids as nutraceuticals: a review. Tropical journal of Pharmaceutical research. 2008. 7(3), pp.1089-1099.
20. Kamiyama M & Shibamoto T. Flavonoids with potent antioxidant activity found in young green barley leaves. Journal of agricultural and food chemistry. 2012. 60(25), 6260-6267.
21. Farshi P. Kaya E C. Hashempour-Baltork F. & Khosravi-Darani K. A comprehensive review on the effect of plant metabolites on coronaviruses: focusing on their molecular docking score and IC50 values.2020 .
22. Das S. Sarmah S. Lyndem S & Singha Roy, A. An investigation into the identification of potential inhibitors of SARS-CoV-2 main protease using molecular docking study. Journal of Biomolecular Structure and Dynamics, (just-accepted). 2020. 1-18.
23. Ganeshpurkar A & Saluja A K. The pharmacological potential of rutin. Saudi pharmaceutical journal. 2017.25(2), 149-164.
24. Das P. Majumder R. Mandal M & Basak P. In-Silico approach for identification of effective and stable inhibitors for COVID-19 main protease (Mpro) from flavonoid based phytochemical

constituents of Calendula officinalis. Journal of Biomolecular Structure and Dynamics. 2020. 1-16.
25. Di Sotto A. Di Giacomo S. Amatore D. Locatelli M. Vitalone A. Toniolo C & Nencioni L. A polyphenol rich extract from Solanum melongena L. DR2 peel exhibits antioxidant properties and anti-herpes simplex virus type 1 activity in vitro. Molecules. 2018. 23(8), 2066.
26. Sun N. Wong W L & Guo J. Prediction of Potential 3CLpro-Targeting Anti-SARS-CoV-2 Compounds from Chinese Medicine.2020 .
27. Paunović S M. Mašković P. Nikolić M & Miletić R. Bioactive compounds and antimicrobial activity of black currant (Ribes nigrum L.) berries and leaves extract obtained by different soil management system. Scientia Horticulturae. 2017.222, 69-75.
28. Rehman S. Ashfaq U A. Ijaz B & Riazuddin S. Anti-hepatitis C virus activity and synergistic effect of Nymphaea alba extracts and bioactive constituents in liver infected cells. Microbial pathogenesis. 2018. 121, 198-209.